STUDIES OF AN EXPERIMENTAL BEAM-STACKING ELECTRON ACCELERATOR

M. Barbier, F. A. Ferger, E. Fischer, P. T. Kirstein, G. L. Munday, M. Morpurgo, M. J. Pentz, A. Schoch, A. Susini and N. Vogt-Nilsen.

CERN, Genève

(presented by M. J. Pentz)

I. INTRODUCTION

The conception of the FFAG type of accelerator (*), which arose independently in at least three places between 1953 and 1956 [1-3], and the idea of beam-stacking in such accelerators [4] or in separate " storage rings " [5] seemed, at the time of the CERN Symposium in 1956, to open up a number of new possibilities in the field of high energy accelerators.

While it has been possible to carry theoretical studies of the processes and phenomena to be expected in a beam-stacking accelerator up to a certain point, there is no doubt that a number of important problems can only be solved by experimental studies with the accelerator itself. This applies particularly to those phenomena which are likely to set the upper limits to the performance. Among these are collective phenomena in high density beams above transition energy [6], interactions between the beam and the RF system during the acceleration and stacking processes [7] and the effects on the stacked beam of radiative energy losses [8] and of space-charge neutralisation [9].

An accelerator intended for experimental studies of these phenomena needs to have a minimum performance and certain design features, which are discussed in Section II of the present paper. Essentially, the accelerator should have a stacking energy in the 100 MeV region and a stacked current of a hundred to several hundred ampere. If it is in addition a two-way machine, it could at the same time provide a means of studying electron-electron scattering at high energy in a centre-of-mass system which is stationary in the laboratory frame.

As a technologically competitive alternative to a two-way FFAG accelerator, we have considered that of a linac and storage rings, basically similar to the scheme under development at Stanford [10], but aimed more at studying high-intensity beams as such than at electron-electron scattering. Although the choice turns out to be primarily an economic one, as may be seen from the discussion in Section II, it is obvious that in some respects such a storage-ring experiment would provide less scope for accelerator research than would the FFAG accelerator.

If the aim is to stack large currents in intersecting beams, it is probable that the linac and storage ring approach is the simplest, though it is not the cheapest. If, however, the aim is also and even primarily to study RF acceleration processes, including possibly methods of crossing transition, and phenomena characteristic of strong-focusing fields, such as radiation anti-damping, then the FFAG alternative must be preferred.

A similar, but inverse, argument applies to the choice between a two-way FFAG and a one-way FFAG. In the latter case one would be free to choose between positive and negative momentum compaction, i.e. positive or negative sign of the magnetic field index; in either case the magnet could be somewhat smaller than with two-way operation. With negative momentum compaction, the possibility

(*) The name is that of the MURA group. Soviet publications use the term " ring phasotron ".

of above-transition space-charge instabilities could be avoided. On the other hand, for the price of a slightly larger accelerator and some additional demands on the injection and RF systems, the two-way alternative does offer the additional attraction of intersecting beam experiments. The fact that it also introduces complications arising from operation above transition is, for an experimental accelerator, not entirely a disadvantage.

In the next section we consider the performance and design features that would be required of a two-way FFAG accelerator intended for the purposes just discussed. We consider what performance might reasonably be expected and where the upper limits might lie. In passing, we consider the limitations of the alternative storage-ring approach.

In the third section we describe the results of some of the design studies in progress at CERN directed towards realising the performance and design features discussed in Section II.

II. PERFORMANCE AND DESIGN FEATURES—REQUIREMENTS, POSSIBILITIES AND LIMITATIONS

1. To study beam-stacking processes

A number of interesting studies of beam-stacking have already been described by the MURA group [11]. So far, these have been at low energy and low intensity in small models, though it is hoped that the 40 MeV two-way model [12] will soon be operating and will allow these studies to be greatly extended. In considering what would be interesting to study in an experimental accelerator which could not be in operation before late 1961, we have had in mind the fact that the MURA two-way model would be in operation considerably earlier, so that it would be desirable to aim at a substantially higher energy and intensity, at which one might expect to encounter phenomena which would be relatively insignificant in the MURA model, but which might be the ultimate limiting factors for this type of accelerator. Three of these phenomena have already been mentioned in the Introduction.

The first, that of "longitudinal" space-charge instabilities above transition energy, has been discussed by Nielsen and Sessler [6]. Taking their formula for the stability criterion of a coasting beam, namely

$$(\Delta E)^2 > \frac{300 g N E_0 e (k+1)(\gamma^2-1)}{\gamma R \pi^2 |k+1-\gamma^2|}, \qquad (1)$$

in which ΔE is the energy spread, in electron-volts, required for stability, of the coasting beam;

g is a geometrical factor dependent upon the beam radius a and the vacuum chamber aperture G, thus: $g = 1+2\ln\frac{2G}{\pi a}$;

N = total number of electrons in the beam;
E_0 = electron rest energy (eV);
e = electron charge (e.s.u.);
γ = E/E_0 where E = electron total energy;
k = magnetic field index;
R = orbit radius (cm).

In the MURA model, injection is to be at 100 keV, transition energy is at 1.64 MeV, and there is to be betatron acceleration to 2 MeV, at which point the RF voltage is adiabatically built up while the frequency modulation is gradually begun[13]. The adiabatic build-up time is to be of the order of 1 millisecond. In the event of the criterion (1) *not* being fulfilled, the build-up time of the longitudinal instability

	MURA 40 MeV	Possible CERN 100 MeV
g	~ 2	~ 2.9
N	$\sim 2\times10^{10}$ to 2×10^{11}	$\sim 10^{12}$ (*)
k	9.3	8
γ	4	4 (*)
R	180 cm	180 cm
$\Delta E >$	~ 4 keV to ~ 12 keV	~ 24 keV

(*) The intention is to inject at 2 MeV (total energy), with a transverse space charge limit of $\sim 3\times10^{13}$: compared with a $\sim 8\times10^{11}$ at 100 keV in the MURA model.

predicted by Nielsen and Sessler would be much shorter than this, perhaps of the order of 1 microsecond. It is interesting to put into formula (1) the parameters of the MURA model at the 2 MeV point, and those at present envisaged for the 100 MeV accelerator being designed at CERN.

The energy spread of the MURA 2 MeV beam is expected to be about 1 keV and has to be less than about 13 keV [13] to stack the required 40 MeV beam with an intrinsic radial spread of < 1 cm. The corresponding figures envisaged for our machine are < 5 keV, and < 25 keV, to stack 100 pulses with an intrinsic radial spread of < 1 cm, assuming a factor of 2 for the loss of phase-space density during capture and acceleration.

Interactions between the electron beam and the RF system would be of two kinds, namely interactions with the accelerated beam on the one hand, or with the stacked beam on the other. As far as we are aware, the former have not yet been studied theoretically. It seems likely, however, that such interactions would become important if the beam loading is comparable with the power dissipated in the unloaded accelerating cavity. The mean power absorbed by the accelerated beam is the product of the accelerated charge, the repetition rate, and the energy difference (expressed in volts) between injection and stacking. The figures for (a) the MURA 40 MeV accelerator and (b) the projected CERN 100 MeV accelerator would be approximately as follows :

	(a) MURA 40 MeV	(b) CERN 100 MeV	
Electrons per pulse	5×10^{10}	10^{12}	
Pulses per sec	60	(i) 100	(ii) 500
Energy gain	38 MeV	98 MeV	
Mean beam loading (*)	2×18 watt	(i) 2×1.6 kW	(ii) 2×8 kW
Unloaded power dissipation in accelerating cavity(-ies)	10 kVA	(i) 3 to 9 kVA	(ii) 16 to 44 kVA (**)

With the higher accelerated charge and higher repetition rate envisaged in our case, beam-cavity interaction is likely to be an important effect, whereas in the MURA accelerator it will be very small.

The most serious problem that will arise from the radiative energy loss of the stacked electron beam will be that of anti-damping of radial betatron oscillations which seems to be inherent in strong-focusing accelerators, at least in the absence of coupling between radial and vertical oscillations [8].

The energy loss per turn of particles moving in the strongly-scalloped orbits characteristic of FFAG accelerators have been calculated by Parzen [14] and by Schoch [15]. With the parameters appropriate to the MURA two-way model at 40 MeV the energy loss per turn is about 3 eV. In the case of our proposed 100 MeV accelerator the corresponding figure would be about 100 eV.

The time constant of exponential growth of radial betatron oscillations would be ~ 3 seconds in the MURA model and $\sim 1/6$ seconds in our case.

The radiated power (which has to be replaced by the RF cavity, or cavities, responsible for maintaining the stacked beam) would in the two cases be ~ 300 watt and ~ 24 kW respectively.

The mean size of the radiated quanta in the two examples would be about 1.5 eV and 24 eV respectively.

Thus it is evident that the quantitative difference between the two cases will give rise to qualitative differences in the devices that will be necessary to deal with radiation losses, and correspondingly in the possibility of testing such devices experimentally.

(*) Simultaneous acceleration of two beams.

(**) Depending upon cavity design, but for two accelerating cavities operating in phase opposition.

In addition to the three phenomena just discussed, which are particularly interesting inasmuch as they might impose limits on the performance of this type of accelerator, there are, of course, others which are partly understood theoretically, have been partly studied in the existing MURA models, and will presumably be studied further in the Two-way Model. These include effects on the RF acceleration and stacking processes of non-adiabatic frequency and voltage changes, errors and misalignments in the RF system, noise and gap voltage harmonics, energy displacement and dispersion of the stacked beam and RF knock-out.

There seems to be no particular disadvantage in studying most of these effects at lower energies and lower beam intensities than we are envisaging, though some might be more pronounced if the RF system is capable of higher acceleration rates.

It is clear, however, that experiments on all these effects would be greatly facilitated by a design which provides relatively good access to the vacuum chamber and which would permit relatively easy and independent variation of parameters. In the design studies we are carrying out at CERN we will have these two requirements very much in mind.

One way in which we hope to meet the first of the two is described in Section III.

2. To study space-charge effects with high currents of relativistic electrons

Budker [9], Linhart [16] and others [17] have discussed the possible equilibrium state of a relativistic self-constricted electron beam when the collision heating of the electron stream is balanced by radiation cooling due to cyclotron oscillations.

The equilibrium criterion is found to be of the form

$$\gamma\nu = \kappa \qquad (2)$$

where the constant κ varies between 2 and 10, depending upon the assumptions made. Here $\gamma = E/E_o$ and ν is the linear density of the electron beam multiplied by the classical electron radius $r_e = e^2/mc^2$.

The quantity of practical interest is not ν but N_s, the total number of stacked electrons, as this number determines the accelerator performance.

If we define an equivalent radius R_s of the stacking orbit in terms of the orbit length $L_s = 2\pi R_s$, then

$$N_s = \frac{2\pi}{r_e}\nu R_s .$$

But R_s is related to the minimum radius of curvature ρ_s of the stacking orbit in terms of the circumference factor C.

$$R_s = C\rho_s .$$

This factor depends upon k and the number of magnet periods M, and upon the azimuthal field flutter function. If we restrict ourselves to a sinusoidal field flutter and to values of k and M that would give approximately equal radial and vertical focusing, the circumference factor C may be treated as approximately constant and of the order of 10, i.e.

$$R_s \sim 10\rho_s .$$

The minimum practicable value of ρ_s is given by the maximum practicable magnetic field strength, since

$$\rho_s B_s \simeq \frac{c}{e/m_0}\gamma_s \text{ for } \gamma_s \gg 1 .$$

Hence

$$N_s \simeq \frac{2\pi}{r_e}\frac{Cc}{(e/m_0)} \cdot \frac{\nu\gamma_s}{B_s} = \frac{2\pi}{r_e}\frac{10c\kappa}{(e/m_0)B_s} . \qquad (3)$$

Thus the number of stacked electrons required to fulfil the condition (2) is approximately constant and independent of the stacking energy.

Numerically, if we take $\kappa \simeq 5$ and a maximum B_s of 10,000 gauss, we find $N_s \simeq 2\times 10^{14}$. This will be an underestimate for energies below about 100 MeV, because one would be compelled by space limitations to use a larger stacking radius than would be obtained with 10 000 gauss, and a correspondingly weaker field.

Theoretical predictions are that a self-constricted relativistic electron beam is likely to be unstable [18], and in addition there would be very great difficulty in replacing the energy lost by cyclotron radiation, whether this would be done by betatron or synchrotron acceleration (in the latter case there would be additional complications due to the bunching of the beam). Consequently we cannot hope to do much more than study some of the incipient processes and possibly the mechanisms of instability.

3. To do electron-electron scattering experiments

The possibility of building a symmetrical two-way FFAG accelerator raises the question of the current density, the energy, and the residual gas pressure required to obtain an electron-electron scattering rate sufficiently large in comparison with background scattering rate. If one uses the Møller formula [19] as a basis for calculation, the electron-electron scattering rate (i.e. the number of electrons scattered per unit solid angle per second per unit length of interacting path) is

$$\sum_{e-e}(\theta) = \frac{c}{2\pi a^2}\left(\frac{N_s}{\pi R_s}\right)^2 \cdot \frac{r_e^2}{4\gamma^2}\left(\frac{1}{\sin^4\theta/2}+\frac{1}{\cos^4\theta/2}+1\right) \quad (4)$$

in which θ is the scattering angle.

With $a = 0.5\,\text{cm}$, $N_s = 10^{14}$, $R_s = 300\,\text{cm}$, $r_e = 2.8\times10^{-13}$ cm, $\gamma = 200$,

$$\sum_{e-e}(\theta) = 105\left(\frac{1}{\sin^4\theta/2}+\frac{1}{\cos^4\theta/2}+1\right)(\text{cm}^{-1}\,\text{sec}^{-1}). \quad (5)$$

The differential cross-section for scattering of electrons on nuclei assuming Coulomb interaction, is given by [19]

$$\frac{d\sigma}{d\omega} = \frac{Z^2 r_e^2}{\sin^4\theta/2}\,\frac{1}{\gamma^2}\left(1-\sin^2\theta/2+ \right.$$
$$\left. + \pi\alpha z(1-\sin\theta/2)\sin\theta/2\right) \quad (6)$$

where Z is the atomic number of the scattering nucleus and α is the fine structure constant, $\left(\alpha \simeq \frac{1}{137}\right)$.

The scattering rate is then

$$\sum_{e-n}(\theta) = \frac{Pn_0N_sc}{\pi R_s}\left[\frac{d}{d\omega}(\theta)+\frac{d}{d\omega}(\pi-\theta)\right] \quad (7)$$

$$= \frac{PZ^2n_0N_sc r_e^2}{\pi R_s\gamma^2}\left[\frac{4}{\sin^2\theta}\left\{\frac{4}{\sin^2\theta}-3-\right.\right.$$
$$\left.\left.-\pi\alpha z\left[1-\frac{2(\sin^3\theta/2+\cos^3\theta/2)}{\sin^3\theta}\right]\right\}\right] \quad (8)$$

in which we assume the scattering gas to be diatomic and where n_o = number of molecules per Torr per cm^3, and P = pressure in Torr. Two terms occur in the bracket because the electron-nucleon background will be contributed to by both beams.

With $P = 10^{-9}$ Torr, $Z = 7$ (nitrogen), $n_0 = 3.6\times10^{16}\,\text{Torr}^{-1}\text{cm}^{-3}$, $N_s = 10^{14}$, $R_s = 300$ cm, $\gamma = 200$

$$\sum_{e-n}(\theta) = 11.0\left[\frac{4}{\sin^2\theta}\left\{\frac{4}{\sin^2\theta}-3-\pi\alpha z\left[1-\right.\right.\right.$$
$$\left.\left.\left.-\frac{2(\sin^3\theta/2+\cos^3\theta/2)}{\sin^3\theta}\right]\right\}\right](\text{cm}^{-1}\,\text{sec}^{-1}). \quad (9)$$

From Eqs. (5) and (8) the ratio

$$\sum_{e-e}(\theta)\Big/\sum_{e-n}(\theta) = \frac{N_s}{8\pi a^2 R_s P n_0 z^2}\cdot\phi(\theta). \quad (10)$$

Although the scattering rate of beam electrons on stationary electrons is larger than either of the above scattering rates, it may be left out of account because the electrons coming from this process will always have much lower energies than will those from the other two, and could easily be distinguished.

The angular dependence of

$$\sum_{e-e}(\theta),\ \sum_{e-n}(\theta) \text{ and } \sum_{e-e}(\theta)/\sum_{e-n}(\theta)$$

is shown in Fig. 1.

It will be observed that with the assumed parameters the ratio is about 10 to 20. The feasibility of the numerical assumptions will be discussed later. The

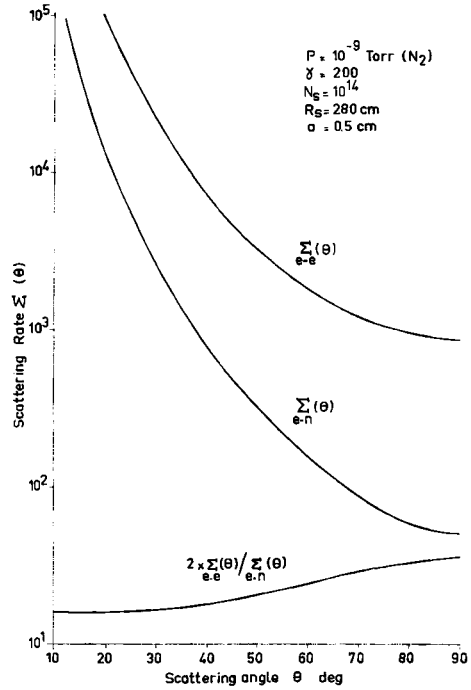

Fig. 1 Electron-electron and electron-nucleus scattering rates

general conclusion is, however, clear enough: a stacked charge of $\sim 10^{14}$ electrons in a 1 cm diameter beam at a residual pressure of 10^{-9} Torr might be just adequate for a 1% experiment on electron-electron scattering. It is true that if radiation damping could be achieved, the ratio (10) could be greatly increased by virtue of the smaller beam diameter. This would, however, mean a correspondingly stronger clearing field.

4. Beam lifetime

For all three purposes discussed above, it is necessary to have a beam with a sufficiently long lifetime—say of the order of 1/10 to 1 second.

Three effects might make this lifetime much shorter. The first, which has already been discussed (in Section II.1), is that of anti-damping of radial betatron oscillations due to radiation. The time for an e-fold increase of amplitude is given by

$$\tau = \frac{10^{-10}}{r_e} \cdot \frac{R_s^2}{F\gamma^3} = 355 \frac{R_s^2}{F\gamma^3} \text{ sec} \qquad (11)$$

where $r_e = 2.82 \times 10^{-13}$ cm and R_s is in cm, and F is a numerical factor to allow for the effect of orbit scalloping on the radiation rate [15].

If it is assumed that R_s is to be increased proportionately to γ in order to limit the maximum magnetic field to a practicable value, then τ is inversely proportional to γ. If we assume, for example, a maximum field of 10 000 G and a radiation factor of 30, we obtain the following time-constants:

Stacking energy MeV	25	50	100	200	300	400	500
Time constant sec (approx.)	2/3	1/3	1/6	1/12	1/18	1/24	1/30

If it is possible to effect radiation damping, or at least a longer build-up time, by means of coupling the radial and vertical betatron motion [8] then the next factor limiting the "single-particle lifetime" would be multiple scattering by the residual gas.

Quite ordinary residual gas pressures, of the order of 1 Torr, would, however, suffice to ensure a scattering lifetime of several seconds at 100 MeV. Since there would be other reasons for requiring much lower pressures than this, the radiation anti-damping effect would seem to be the important one in practice.

However, in order to avoid instabilities due to space-charge neutralisation, it would be necessary to have an electrostatic clearing field to remove positive ions created in the electron beam. The necessity for this may be seen from the following simple calculation.

Fermi [20] gives figures for the energy loss due to ionisation by relativistic electrons in air, and for the energy spent per ion pair created. These figures show that 100 MeV electrons produce about 1.3×10^{-10} ion pairs per cm in air at 10^{-9} Torr. Thus a beam of 10^{14} electrons would produce $3 \times 10^{10} \times 10^{14} \times 1.3 \times 10^{-10} \simeq 4 \times 10^{14}$ ion pairs per second. Hence the time required to produce neutralisation of the relativistic beam (i.e. to produce $10^{14}/\gamma_{\prime\prime}^2$ ion pairs) would be about $1/(4\gamma_{\prime\prime}^2)$ sec or ~ 25 μsec at 100 MeV.(*)

The field required is

$$E_z = \frac{60I}{Q} = 4.6 \times 10^{-8} \frac{N_s}{aR_s} \text{ volt cm}^{-1}$$

where

I = electron current, in ampere, a = cross-sectional radius of electron beam, in cm. Thus, for example, with $N_s = 10^{14}$, $a = 1.0$ cm, $R_s = 300$ cm, $E_z \simeq 15$ kV per cm. Such a field would be equivalent to a radial magnetic field $B_r = E_z/300 \simeq 50$ G, which is equivalent to a vertical magnet displacement $\Delta z = R_s B_r / k B_z$ cm. With $R_s = 300$ cm, $B_r = 50$ G, $k = 8$ and $B_z = 10\,000$ G, $\Delta z \simeq 1.87$ mm.

The power required from the high-voltage generator supplying the clearing field may be estimated as follows.

Clearing electrode current $= 2 \times 4 \times 10^{14} \times 1.6 \times 10^{-19}$ $= 128$ μA. Assuming an electrode spacing of 10 cm, i.e. a voltage of 150 kV, the power is then ~ 19 W.

If, however, the pressure were only 10^{-6} Torr the clearing current would be 128 mA and the power 19 kW.

(*) Here $\gamma_{\prime\prime} = (1 - V_{\prime\prime}^2/c^2)^{-1/2}$, where $V_{\prime\prime}$ is the average velocity in the direction of the beam. This may be calculated from the orbit radius, the frequency and amplitude x of betatron oscillations and the energy. With $\gamma = 200$, $R_s = 300$ cm, $Q_R = 6$, $x = 1$ cm, $\gamma_{\prime\prime} \sim 130$; and with $x = 2$ cm, $\gamma_{\prime\prime} \sim 77$. We accordingly take $\gamma_{\prime\prime} \sim 100$.

Summary of requirements

1) Experiments on beam-stacking: injected charge 10^{11} to 10^{12} electrons; repetition rate 100 to 500 pulses per second; positive momentum compaction; stacking energy 50 to 100 MeV; single-particle life 0.1 to 1 sec.
2) Experiments on space-charge neutralized beams: stacked charge $\sim 10^{14}$ electrons, single-particle life 0.1 to 1 sec; residual gas pressure $\sim 10^{-9}$ Torr; beam diameter ~ 1 cm.
3) Experiments on electron-electron scattering: stacked charge $\sim 10^{14}$ electrons; beam lifetime ~ 1 sec; residual pressure $\sim 10^{-9}$ Torr; beam diameter ~ 1 cm.

We now consider whether such requirements would be feasible, and how far they might be exceeded.

5. Possibilities and limitations

(a) The injected charge

The limiting factors will be the transverse space-charge limit in the inflected beam, the space-charge and other limits in the injector, and the efficiency of the inflection process.

As is well-known, the effect of space-charge on the particle motion is to weaken the focusing forces and thus decrease the betatron wave numbers Q_R and Q_z. During the acceleration the space charge forces decrease rapidly with increasing energy and so the Q's will increase to the " single-particle " values. The operating point must not be allowed to cross a resonance line in the process. This restricts the change in Q, $\Delta Q < \sim 1/5$. The maximum number of electrons round the orbit at injection is then given by

$$N_i < \frac{2\pi a^2 Q}{5 R_i r_e} \gamma_i^3 \beta_i^2 \qquad (12)$$

where R_i is the injection orbit radius; a the cross-sectional radius of the injected beam; Q the radial or vertical betatron wave-number (assumed to be equal); $\gamma_i = E_i/E_o$, where E_i = total injection energy and E_o the rest energy; $\beta_i = v_i/c$, where v_i is the velocity of the injected electron; and r_e is the classical radius of the electron.

With $a = 1$ cm, $Q = 6$, $\gamma_i = 4$ ($E_i \simeq 2$ MeV), $\beta_i \simeq 1$, $R_i \simeq 200$ cm (corresponding to $R_s = 300$ cm, $k \simeq 8$), $r_e = 2.8 \times 10^{-13}$ cm.

$$N_i < 3 \times 10^{13}/\pi \lesssim 10^{13}$$

The aim of 10^{12} electrons would thus be well within this limit.

If " the inflection process " is taken to mean the inflection of the beam in such a way as to allow a proportion of it to miss the inflector, plus the capture of some of that inflected beam into an accelerating bucket, then we do not yet know enough to be able to predict an " efficiency " for this process. If, in addition, collective interactions have to be taken into account, the inflection process as a whole becomes extremely complicated, and one doubts whether a useful theoretical solution is indeed possible.

A simple, linear, one-particle study of inflection with a programmed field bump has been made on the CERN Mercury Computer, and indicates that it might be possible to inflect a considerable fraction of 20 turns with the parameters we are envisaging. This would correspond to an injection pulse length of about 0.8 μsec.

If we allow an arbitrary factor of 10 for the inefficiency of the inflection process, the injector current would then be $10^{13} \times 1.6 \times 10^{-19}/0.8 \times 10^{-6} = 2$ A.

The energy spread of this beam has to be limited, as it contributes to the energy spread of the final stacked beam. A spread of 3 MeV at 100 MeV (corresponding to a radial spread of 1 cm in 300 cm if k is 8) would require an energy spread at injection < 25 keV, assuming a phase space density loss of 2 during acceleration. The inflection computations referred to above assumed a beam divergence of 10^{-3}, which is probably near the limit achievable with a 2 A, 2 MeV beam.

The requirement of 4 ampere (two beams) with less than 25 keV energy spread seems to be within the capability of a Van de Graaff generator, if a method can be found to compensate for the terminal voltage droop during the injection pulse, which might otherwise be about 40 kV.

(b) The lifetime of the stacked beam

As has been mentioned in Section II.1, the lifetime will be limited mainly by radiation anti-damping, and would be about 0.5 sec at 100 MeV. The necessary provision of clearing fields of ~ 15 kV/cm would be technically feasible. The maintenance of the beam for this time, or even longer if the radiation anti-damping effect can be successfully overcome,

implies an RF cavity, or cavities, to replace the average energy loss of the stacked beam which would be about 100 volts per turn for 100 MeV orbits with a radiation factor of 30, or about 1500 MeV per sec.

In principle two methods exist for doing this. One is to modulate empty buckets through the stacked beam from above, thereby displacing it upwards in energy. The other is to hold the whole stacked beam in a synchronous bucket of large amplitude.

The repetition frequency m with which a displacement bucket must be modulated through the stacked beam in order to replace an energy loss ε MeV per turn may be calculated from the formula :

$$m^2 = \frac{\pi^3 f_s^3 \varepsilon^2 \Gamma \Delta t}{32 \Delta E_s (k+1) E_s \alpha^2(\Gamma)} \tag{13}$$

where

f_s = revolution frequency of stacked electrons,

Γ = phase parameter of displacement bucket

$\alpha(\Gamma)$ = a function of Γ (see Fig. 14 in Symon and Sessler [4], or Eq. (71) in Vogt-Nilsen [22]),

ΔE_s = energy range through which displacement bucket is modulated,

Δt = time for bucket to be modulated linearly through the interval ΔE_s

(Because of finite recycling time $1/\Delta t > m$; for instance we might take $1/\Delta t = 2$ m.)

The peak voltage required for this displacement bucket is given by

$$V = \frac{\Delta E_s}{\Gamma f_s \Delta t} . \tag{14}$$

Formulae (13) and (14) may be used to find an optimum value for Γ, such that V is a minimum.

For example, with $\varepsilon = 10^{-4}$ MeV, $f_s = 2 \times 10^7$ sec^{-1}, $\Delta E_s = 4$ MeV, $E_s = 100$ MeV, $k = 7$, and $1/\Delta t = 2m$ we find the following

Γ	0.1	0.2	0.3	0.4	0.5	0.6	0.7	0.8
m sec^{-1}	124	178	234	299	382	497	676	1005
V volts	495	356	312	299	306	332	386	502

For the second method, the voltage per turn to be provided by the cavity or cavities may be calculated from the requirement that the bucket area should be at least equal to the phase space area occupied by the stacked beam.

Then

$$V \geq \frac{\pi^3}{32} \frac{\Delta E_s^2}{E_s(k+1)} . \tag{15}$$

With $\Delta E_s = 4$ MeV, $E_s = 100$ MeV and $(k+1) = 8$ as in the previous example, we find

$$V \geq 19.4 \text{ kV} .$$

Measurements we have made on a full-scale model cavity operating in the 20 to 30 mc/s range show that the unloaded shunt impedance is about 2 000 ohm. Thus if two such cavities were used for beam maintaining, with 10 kV peak on each, a total radio-frequency power of 58 kW would be needed, and this would be as expensive as the power for acceleration at the limit of 500 pulses per second.

In any case it might be necessary to use the displacement method during the acceleration and stacking process, because the large RF forces of the stationary bucket might otherwise simply remove the electrons from the accelerating buckets. On the other hand, the displacement method involves a certain amount of energy dispersion of the stacked beam, so that, cost aside, there might be some value in using displacement only during the stacking and a large stationary bucket subsequently.

(c) The repetition rate

To stack 10^{14} electrons in a time of 0.5 seconds with 10^{12} electrons per pulse means a repetition rate of 200 pulses per second. If it were possible for the accelerating voltage to be at its maximum value throughout the whole 5 millisecond cycle, the peak voltage required would be 800 V per turn. Since the accelerating voltage must be increased adiabatically a factor of at least 1.5 should be allowed; hence about 1.2 kV per turn would be more realistic. This might, for example, be provided by two diametrically opposite cavities operating in anti-phase with a peak voltage of 600 V each. Since the frequency modulation ratio with $k \simeq 8$ is about 1.5 (assuming injection at 2 MeV) the cavity Q would have to be reduced by loading to about 4, which would correspond to a shunt impedance at resonance $R_p \simeq 60$ ohm, with the cavity geometry imposed by the restriction on magnet radii implied by a maximum magnetic field of about 10 000 G.

Such a cavity would dissipate 3 kW in its resistive load. In addition, the two accelerated beams would

constitute a load of 4.8 kW on each of the two cavities. The total cavity power would thus be 15.6 kW (two cavities).

If the acceleration rate is increased to 500 pulses a second, the total cavity power would become 61.5 kW. The latter figure is near the practical limit, and we would estimate the cost of the RF power installation to be about 350 000 Swiss francs.

In the preceding calculations we have been assuming an injection energy of 2 MeV and a final energy of 100 MeV. It is instructive to estimate the feasibility and cost of going to a higher final energy.

(d) Effect of increasing the final energy

The overriding limitation to the final energy is the radiated energy lost by the stacked beam. At 100 MeV, with 10^{14} stacked electrons per beam and $R_s = 333$ cm (corresponding to a maximum field of 10 000 G and a circonference factor of 10), the average power radiated is 21 kW by each beam. At 200 MeV, if one keeps the maximum field constant, and therefore doubles the radius, the radiated power is 8 times larger, or 336 kW for both beams. In order to try to halve this loss (for instance) by doubling the radius, it would be necessary to double the stacked charge in order to maintain the same $\nu\gamma$ (Equation 2) or the same ratio of scattering rates $\sum_{e-e}(\theta)/\sum_{e-n}(\theta)$ (Eq. 10) and this would in turn double the radiated power again. Even if it were technically feasible to supply this order of power to maintain the beam, the increased cost of the RF system, the magnet, the vacuum system and the accelerator building would, as a very rough estimate, bring the cost of such an accelerator well above 30 million Swiss Francs (excluding salaries of staff), or more than four times the estimated cost at 100 MeV. In view of the very much greater technical difficulties, the additional cost of man-hours of development and construction would bring the total up to nearer five times greater.

In this connection it is relevant to consider the alternative of a linear accelerator with weak-focusing storage rings, as in the Princeton-Stanford project [10]. The radiation loss would then be about ten times less for the same magnet radius and electron energy (because of the absence of strong scalloping of the orbits).

On the basis of figures quoted for a 40 MeV electron linear accelerator [21] one might guess the cost of a 100 MeV electron linac to be about 10 million Swiss francs. To this would have to be added the cost of the storage rings, RF system, vacuum system, etc., which could amount to about 3 million Swiss francs, and a million for the building would bring the total up to 14 million, or about 2½ times the estimated cost of a 100 MeV beam-stacking accelerator. The difference would probably be less at 200 MeV, and at higher energies still, the linac and storage ring combination would become less expensive than the beam-stacking FFAG.

We conclude that this type of beam stacking accelerator can not be extended, within reasonable technical and economic limitations, to much higher energies than 100 MeV, at which level it is much more economical than any other device of comparable performance, and that it would be possible at this energy, and with a stacked charge of about 10^{14} electrons, to perform useful experiments on beam-stacking at high intensity, on space-charge phenomena, and in quantum electrodynamics.

III. DESIGN STUDIES AT CERN

In this section we report on two features of the design studies in progress at CERN and directed towards the design of a 100 MeV two-way beam-stacking accelerator. These features are chosen for comment because they seem to be new developments which, though quite modest in themselves, might permit considerable improvements in the design. These are : 1) the development of a magnet of simple construction and with horizontal return yokes and an open median plane, and 2) the introduction of superperiods into radial-sector FFAG structures.

1. Horizontal yoke magnet

We have constructed a 1 in 2.5 scale model of two sectors of a magnet with 10 pole pairs ($M = 10$) and $k = 7$.

A drawing of one sector is shown in Fig. 2 and photographs of an assembled sector, and of the separate halves of a sector are shown in Fig. 3 and Fig. 4.

It will be seen that the return flux goes through a horizontal yoke instead of a vertical yoke as in

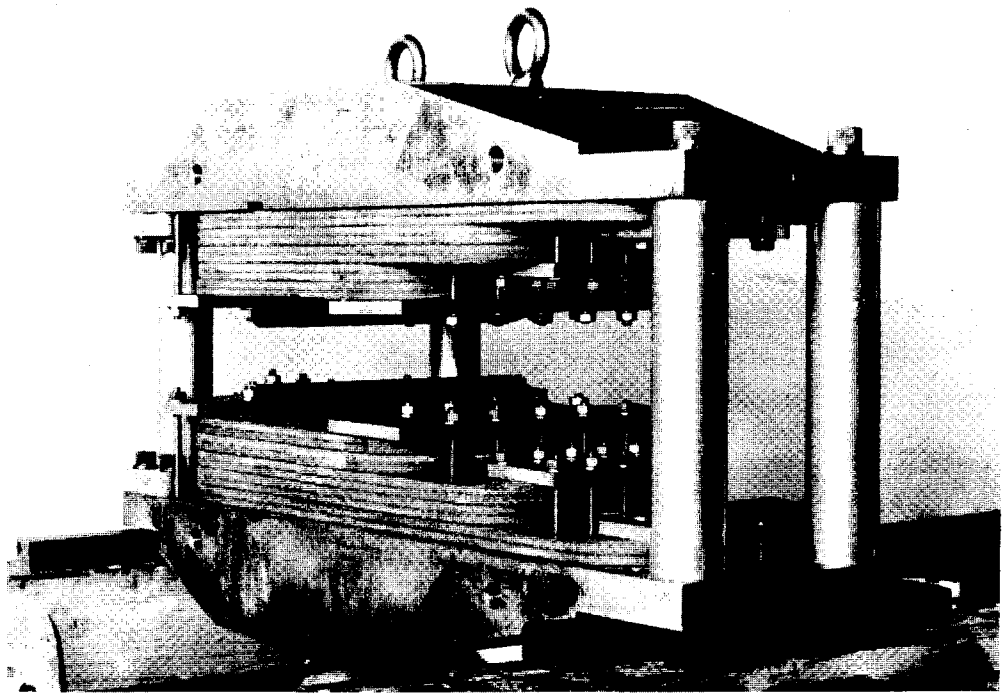

Fig. 3 One sector of the magnet model.

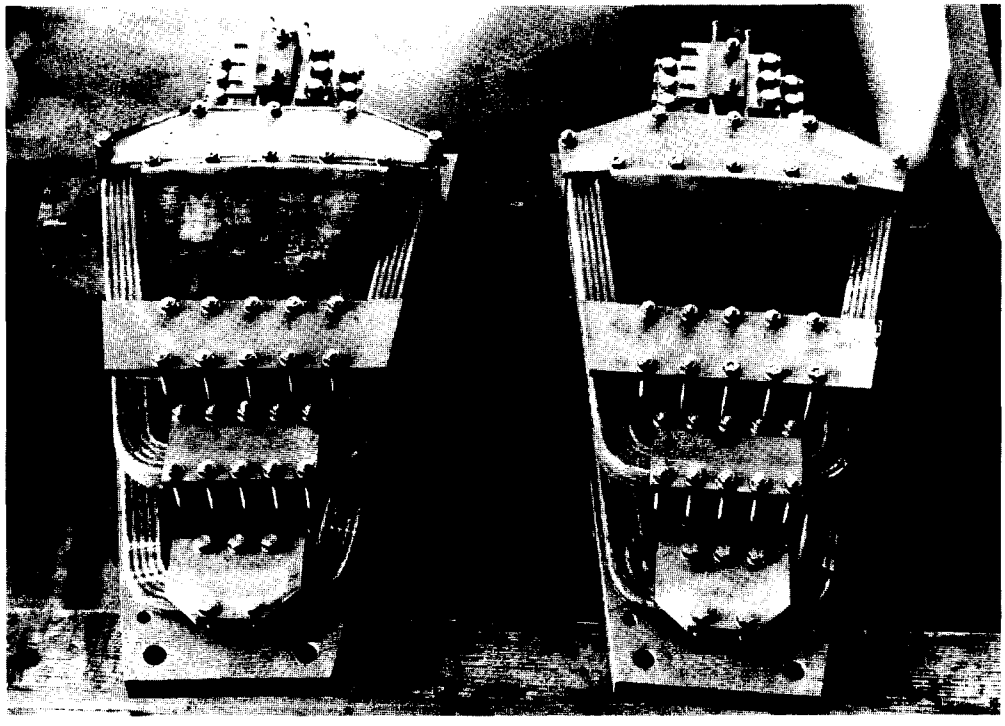

Fig. 4 Upper and lower halves of one sector of the magnet model.

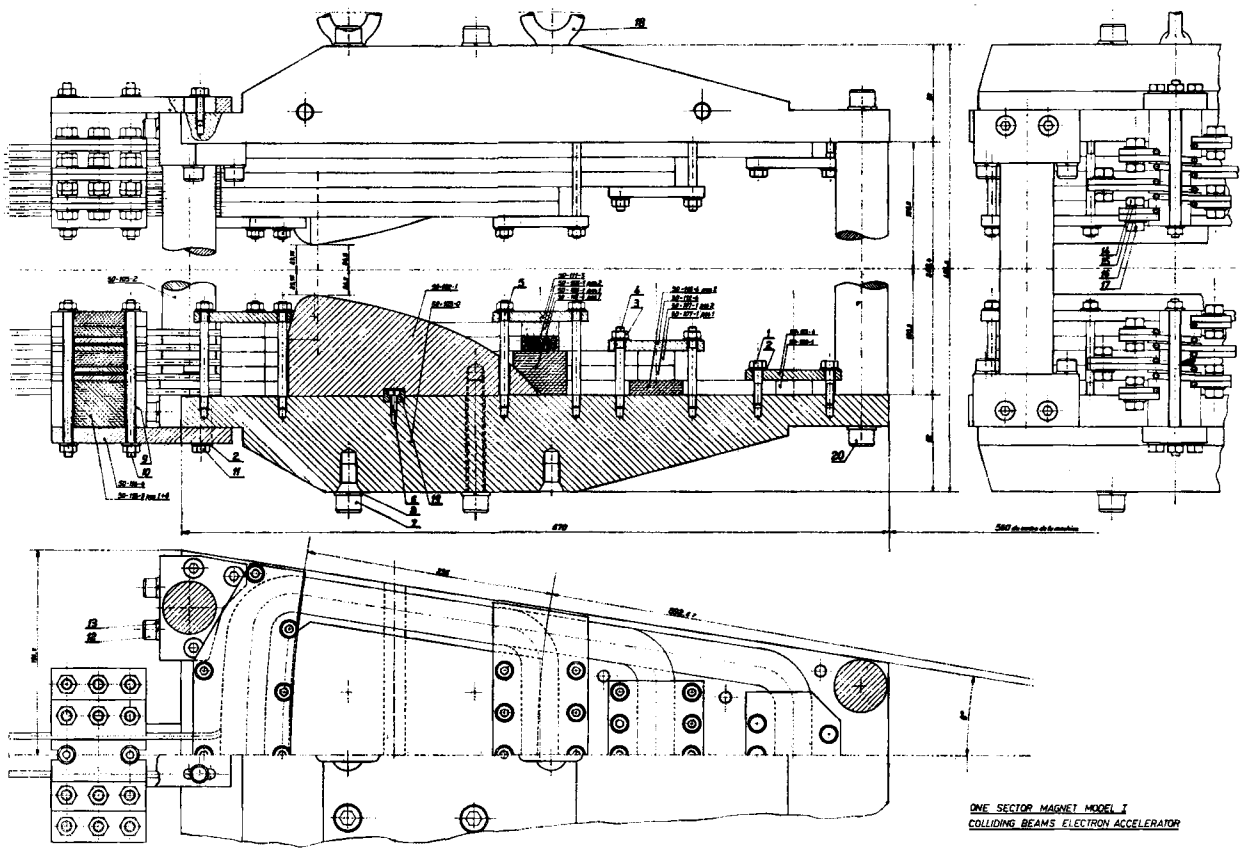

Fig. 2 Magnet model. 1/2.5 times full size.

the MURA 40 MeV model. This has the advantage of good access to the vacuum chamber, and in particular a median plane easily accessible from both inside and outside.

A continuous ring structure as shown schematically in Fig. 5 would, of course, leave no gaps for the insertion of accelerating cavities (*). If, however, the structure is broken in a number (necessarily an even number for two-way symmetry) of planes of symmetry in the azimuthal field configuration, i.e. in the centres of a number of magnet poles, then there is still no need for additional yokes, whether vertical or horizontal, to return the flux. This is shown schematically in Fig. 6.

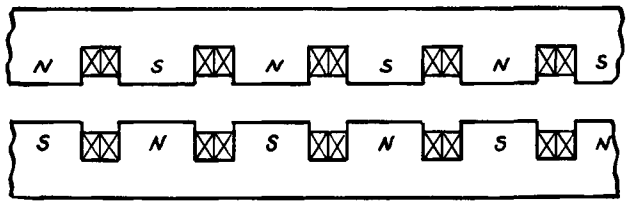

Fig. 5 Magnet with continuous ring yokes.

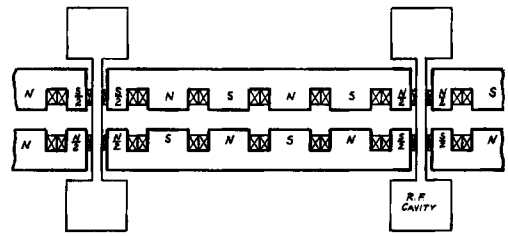

Fig. 6 Azimuthal gaps at symmetry planes to accommodate accelerating cavities.

(*) The possibility of drift tubes or " dees " entirely inside the vacuum chamber is being considered, as this would obviate any necessity to break the magnet yokes, and might prove useful if the large insulating vacuum seals for the cavities cannot be made. However, the RF power required would be still higher than with cavities.

This would introduce a superperiod into the magnet structure and therefore (unless special measures were taken to avoid it) into the azimuthal field configuration. The results of digital computer studies of the electron orbits in such field configurations are reported in Section III.2.

Another feature of the magnet model shown in Figs. 2 to 4 is the very simple coil arrangement. In order that the magnet should be easy to put together and take apart it is desirable that the coils should be removable and replaceable by simple operations. For this it is best to have each group of turns in a coil lying in one plane.

Studies were made with a stainless steel plate analogue [23] to arrive at the radial profile of the pole-pieces and the positions of the backwindings required to give a seventh power law of radial variation of the field.

The first series of magnetic field measurements made on the model gave the results shown in Figs. 7 and 8. Fig. 7 shows the variation of $k = \frac{R}{B}\cdot\frac{dB}{dR}$ with radius. Considering the extreme simplicity of the coil arrangement, we think this result is quite promising. A computer programme has now been developed which will be used to guide the process of subdivision and distribution of the coils which will be made in the next stage of development of the model.

Fig. 8 shows the azimuthal variation of the field, normalized at the pole centre, for different radii. The smallest radius, 65 cm, corresponds to about 17 cm inside the injection radius (180 cm) and the largest, 110 cm, corresponds to about 5 cm outside stacking radius (270 cm) in the full-scale version. At the smaller radii, the field is very close to sinusoidal.

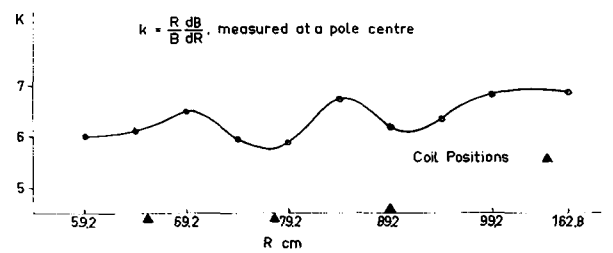

Fig. 7 Field index measured along a radius at the azimuthal centre of a pole in the magnet model.

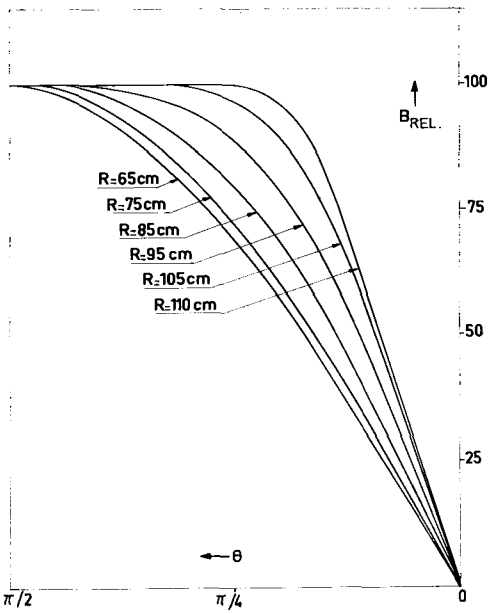

Fig. 8 Normalised azimuthal field variation measured at different radii in the magnet model.

Computer studies were made of the linear betatron oscillations of electrons in fully-scaling fields corresponding to the azimuthal variations shown in Fig. 8. These results are summarised in Fig. 9 for the case of a magnet with (a) 14 pole pairs, (b) 15 pole pairs.

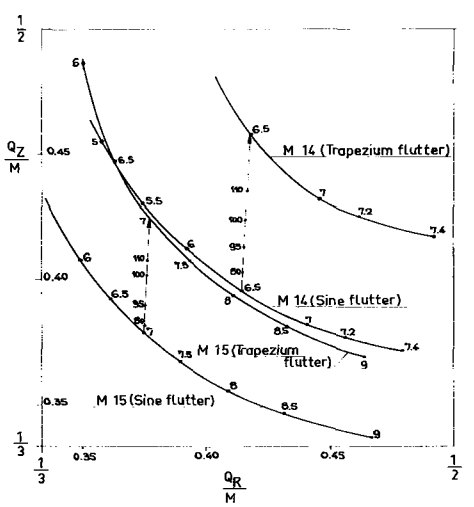

Fig. 9 The figure shows the results of computations of Q_z and Q_R for $M = 14$ and $k = 5$ to 7.4, and for $M = 15$ and $k = 6$ to 9. In each case a sinusoidal flutter function and a sharp trapezium flutter function were employed. The latter approximated, except for the sharp edges, to the field measured at radius 110 cm in the magnet model. With the actual field flutters measured on the model at 80 cm, 95 cm, 100 cm and 110 cm the computed Q-values for $M = 14$, $k = 6.5$ and for $M = 15$, $k = 7$ were as shown in the figure.

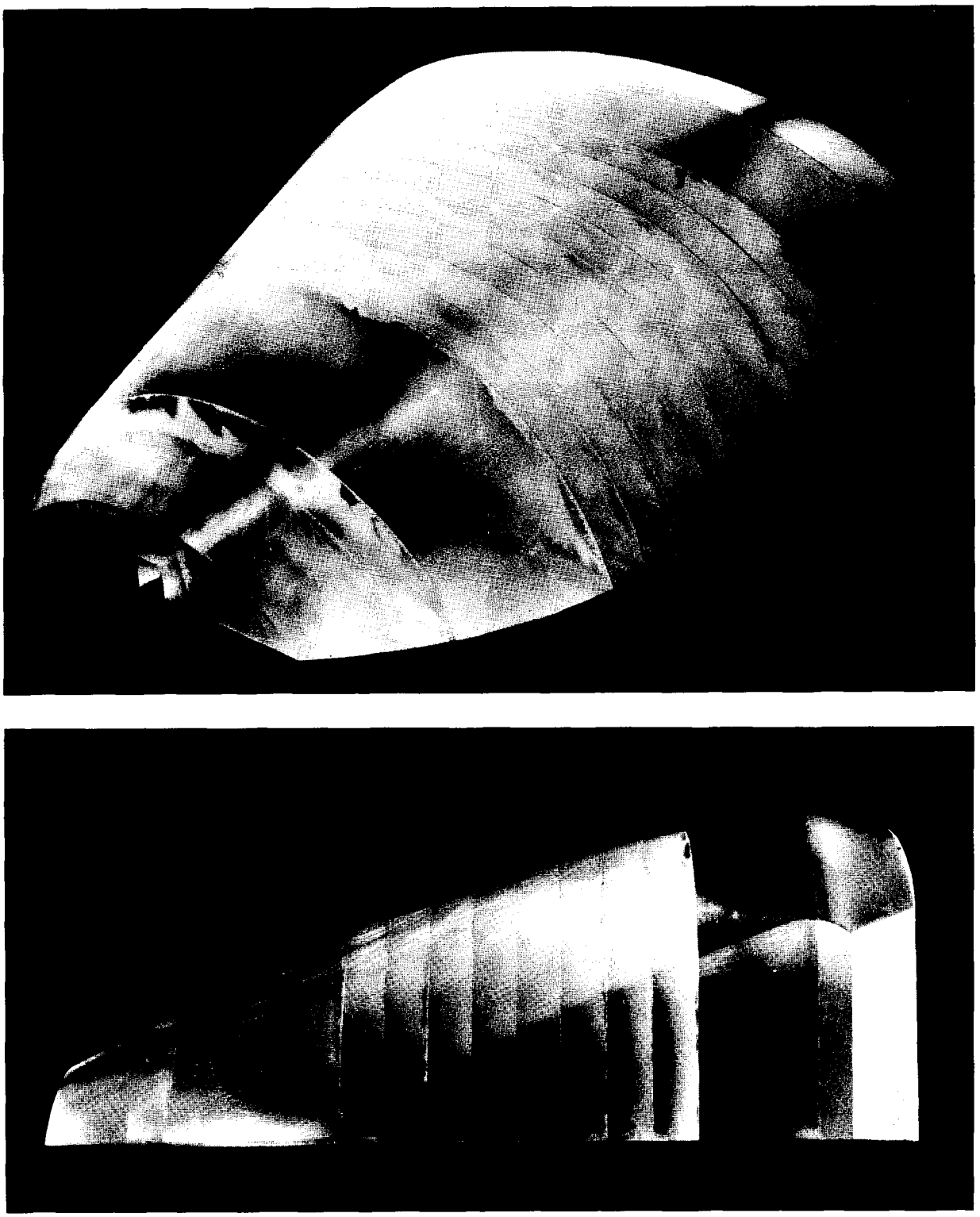

Fig. 10 Perspex templates for profiled pole-pieces.

It can be seen that the form of the flutter function affects mainly the vertical focusing, as is to be expected.

Following these preliminary studies, the azimuthal profiles of the pole pieces required to fit the equipotential surfaces corresponding to a nearly sinusoidal flutter at all radii, were determined with the help of the Mercury Computer, and profiled pole-pieces are at present being manufactured. The perspex templates for these are shown in the photographs in Fig. 10.

It is expected that with further distribution of the backwindings and with the profiled poles it will be possible to make k constant to within 1% and to maintain a sufficiently constant flutter function at all radii to ensure that the operating point Q_R, Q_Z is sufficiently defined and fixed.

Future studies on the magnet model will include the problem of producing scaling fields in the straight sections.

2. Orbits in FFAG fields with superperiods

We have developed computer programmes for use with the CERN Mercury Computer which allow us to find the non-linear orbits and stability limits in the median plane and the linear radial and vertical betatron oscillation frequencies.

Any periodic azimuthal field configuration can be used, but it is assumed that this configuration scales, i.e. it is the same at all radii.

We have considered various ways of introducing superperiods into a sinusoidal configuration, and have just recently begun to obtain some positive results for a particular case. The field configuration studied is as indicated in Fig. 11, showing the angular field flutter function.

The interval BA in the figure represents one quarter period of the structure, i.e. one-eighth of the whole magnet. It contains nine quarter sine waves, plus a single region where the field is zero. There are thus 4½ magnet poles per quarter period. The magnet period is obtained by repeating the field configuration BA by reflecting it once about a plane of symmetry (such as $A - A$), and then reflecting the resulting configuration once about a plane of asymmetry. There are $M = 2$ superperiods around the magnet circumference, each containing 2 zero field sections and 18 poles. There are accordingly 18 pole pairs around the whole magnet. We characterize this structure by the label $M = 2$ (18).

This structure is of course an unrealistic simplification. In practice the field in the straight section would not go to zero, and might indeed be only slightly depressed if the straight section is short. The effect on the orbits of such a real field is likely to be much less pronounced than that of the idealized zero-field sections we have studied up to the present moment. The results are all the more encouraging for that.

In the appendix is given the complete set of equations upon which our study of orbit dynamics has been based. Only very preliminary results can be reported at the present stage. In Fig. 12 the two wave numbers are given as a function of the field index k for the $M = 2$ (18) machine having sharp edge zero field straight sections of the length 1/7

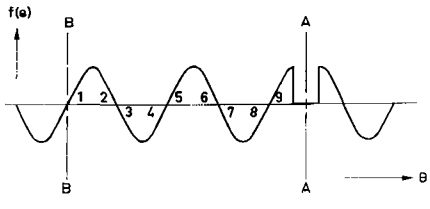

Fig. 11 Field configuration for digital computer studies of orbits in FFAG field with superperiods.

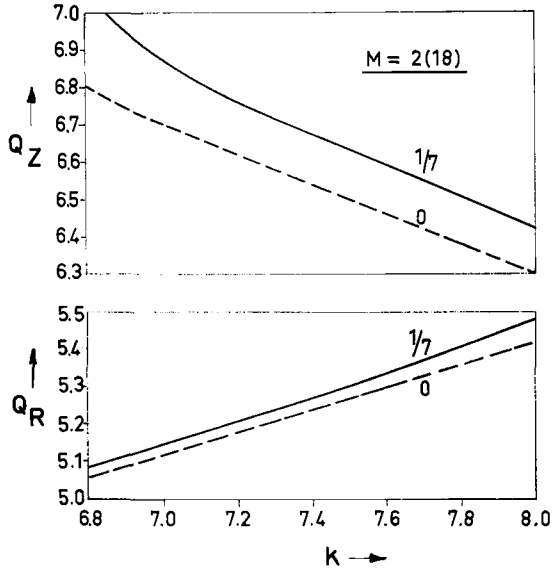

Fig. 12 Dependence of betatron frequencies upon field index with field configuration of Fig. 11.

of a magnet pole. For comparison, the dotted curves for the corresponding machine without any straight sections are also shown. It is seen that at least in this case no drastic changes in the wave numbers occur by the introduction of sraight sections. By a crude test involving orbits going three times round the machine, it is indicated that the extent of the radially stable region at the position of the straight section is about 5.7% of the radius for $k = 7$ and about 3.8% for $k = 8$. This is to be compared with 9.6% at a comparable position in a machine with no straight sections and with $k = 7$. These limits of stability are considered adequate for our purposes. The vertical stability limits have not yet been considered.

APPENDIX

The magnetic field structure for the machine under consideration has been described in terms of cylindrical coordinates (r, θ, z). The defining boundary conditions on the median plane $z = 0$ are chosen in the form

$$\begin{aligned} B_r(r,\theta,0) &= B_\theta(r,\theta,0) = 0 \\ B_z(r,\theta,0) &= B_0\left(\frac{r}{r_0}\right)^k f(\theta) \end{aligned} \tag{A.1}$$

where r_0, B_0 are positive constants, k the field index and $f(\theta)$ the azimuthal field flutter function. The sign convention is chosen such that an electron circulating in the positive direction will experience a deviation towards the machine axis in the sectors of positive $f(\theta)$.

The magnetic field satisfying the conditions (A.1) may be expressed as the series :

$$\begin{aligned} B_r &= -B_0\left(\frac{r}{r_0}\right)^k \sum_{j=1}^{\infty} 2j(k+2-2j) \sum_{\alpha=1}^{j} C_{j,\alpha} f^{(2\alpha-2)} \left(\frac{z}{r}\right)^{2j-1} \\ B_\theta &= -B_0\left(\frac{r}{r_0}\right)^k \sum_{j=1}^{\infty} 2j \sum_{\alpha=1}^{j} C_{j,\alpha} f^{(2\alpha-1)} \left(\frac{z}{r}\right)^{2j-1} \\ B_z &= -B_0\left(\frac{r}{r_0}\right)^k \sum_{j=0}^{\infty} (2j+1)(2j+2) \sum_{\alpha=0}^{j} C_{j+1,\alpha+1} f^{(2\alpha)} \left(\frac{z}{r}\right)^{2j} \end{aligned} \tag{A.2}$$

where the coefficients $C_{j,\alpha}$ ($j = 1, 2, \ldots, \alpha = 1, 2, \ldots, j$) dependent only on the field index are derivable from the recursion formulas

$$C_{1,1} = -\frac{1}{2} \qquad C_{2,1} = \frac{k^2}{4!} \qquad C_{2,2} = \frac{1}{4!}$$

$$\left.\begin{aligned} C_{j,1} &= -\frac{(k+4-2j)^2}{2j(2j-1)} C_{j-1,1} \\ C_{j,\alpha} &= -\frac{(k+4-2j)^2 C_{j-1,\alpha} + C_{j-1,\alpha-1}}{2j(2j-1)} \\ &\qquad (\alpha = 2, 3, \ldots, j-1) \\ C_{j,j} &= \frac{(-1)^j}{(2j)!} \end{aligned}\right\} (j = 3, 4, 5, \ldots) \tag{A.3}$$

and the notation $f^{(\alpha)} = \dfrac{d^\alpha f}{d\theta^\alpha}$ is used.

The orbital equations are expressed in terms of the scaled variables

$$\rho = \frac{r}{S(p)}, \quad \zeta = \frac{z}{S(p)} \tag{A.4}$$

where the scale factor $S(p)$ is determined by the momentum $p = mv$ of the electron under consideration according to the formula

$$S(p) = r_0 \sqrt[k+1]{\frac{p}{eB_0 r_0}}. \tag{A.5}$$

The orbital equations are then derivable from the Hamiltonian

$$\begin{aligned} H &= \mp\rho\Phi - U_4 \\ \Phi &= \left[1-(p_\rho - U_1)^2 - p_\zeta^2\right] \end{aligned} \tag{A.6}$$

i.e.

$$\begin{aligned} \rho' &= \pm\frac{\rho}{\Phi}(p_\rho - U_1) \\ p'_\rho &= \pm\Phi \pm \frac{\rho}{\Phi}(p_\rho - U_1)U_2 + U_5 \\ \zeta' &= \pm\frac{\rho}{\Phi} p_\zeta \\ p'_\zeta &= \pm\frac{\rho}{\Phi}(p_\rho - U_1)U_3 + U_6 . \end{aligned} \tag{A.7}$$

Here the double sign corresponds to a motion in the positive or negative angular direction respectively, the primes denote differentiation with respect to θ and

$$U_1 = \rho^{k+1} \sum_{j=1}^{\infty} \sum_{\alpha=1}^{j} C_{j,\alpha} f^{(2\alpha-1)} \left(\frac{\zeta}{\rho}\right)^{2j}$$

$$U_2 = \rho^{k} \sum_{j=1}^{\infty} (k+1-2j) \sum_{\alpha=1}^{j} C_{j,\alpha} f^{(2\alpha-1)} \left(\frac{\zeta}{\rho}\right)^{2j}$$

$$U_3 = \rho^{k} \sum_{j=1}^{\infty} 2j \sum_{\alpha=1}^{j} C_{j,\alpha} f^{(2\alpha-1)} \left(\frac{\zeta}{\rho}\right)^{2j-1} \qquad \text{(A.8)}$$

$$U_4 = -\rho^{k+2} \left[\frac{f}{k+2} + \sum_{j=1}^{\infty} (k+2-2j) \sum_{\alpha=1}^{j} C_{j,\alpha} f^{(2\alpha-2)} \left(\frac{\zeta}{\rho}\right)^{2j} \right]$$

$$U_5 = -\rho^{k+1} \left[f + \sum_{j=1}^{\infty} (k+2-2j)^2 \sum_{\alpha=1}^{j} C_{j,\alpha} f^{(2\alpha-2)} \left(\frac{\zeta}{\rho}\right)^{2j} \right]$$

$$U_6 = -\rho^{k+1} \sum_{j=1}^{\infty} 2j(k+2-2j) \sum_{\alpha=1}^{j} C_{j,\alpha} f^{(2\alpha-2)} \left(\frac{\zeta}{\rho}\right)^{2j-1} .$$

On the median plane the orbital equations reduce to

$$\rho' = \pm \frac{\rho}{\Psi} p_\rho$$

$$p'_\rho = \pm \Psi - \rho^{k+1} f \qquad \Psi = \sqrt{1 - p_\rho^2} \qquad \text{(A.9)}$$

The scaled equilibrium orbit is described by the periodic solution of Eqs. (A.9) with the period $2\pi/M$ of the magnetic field structure. Denoting this solution by $\bar{\rho}$, $\bar{p}_\rho$ the equations describing the linearized betatron oscillations in the relative coordinates

$$x = \rho - \bar{\rho}\,, \quad y = \zeta$$
$$p_x = p_\rho - \bar{p}_\rho\,, \quad p_y = p_\zeta \qquad \text{(A.10)}$$

are

$$x' = \pm \frac{\bar{p}_\rho}{\bar{\Psi}} x \pm \frac{\bar{\rho}}{\bar{\Psi}^3} p_x$$

$$p'_x = -(k+1) f \bar{\rho}^{-k} x \mp \frac{\bar{p}_\rho}{\bar{\Psi}} p_x \qquad \text{(A.11)}$$

$$y' = \pm \frac{\bar{\rho}}{\bar{\Psi}} p_y$$

$$p'_y = \bar{\rho}^{-k} \left(kf \mp \frac{\bar{p}_\rho}{\bar{\Psi}} f' \right) y$$

where $\bar{\Psi} = \sqrt{1 - \bar{p}_\rho^2}$. These equations allow one to determine the wave numbers Q_R, Q_Z without having to solve the more complicated general equations (A.7)

A number of digital computer programmes based on the above equations have been developed. By means of these an extensive study of the orbit dynamics relevant to the proposed type of accelerator is in progress. A few preliminary results are given in Section III.2.

LIST OF REFERENCES

1. Kolomenskij, A. A., Petukhov, V. A. and Rabinovich, M. S. Report of the Lebedev Physical Institute of the USSR Academy of Sciences. 1953. Moscow.
2. Kerst, D. W., Symon, K. R., Laslett, L. J., Jones, L. W. and Terwilliger, E. M. Fixed field alternating gradient particle accelerators. CERN Symp. 1956. *1*, p. 32-5.
3. Private communication from T. Ohkawa. University of Tokyo, Tokyo, Japan. 1953.
4. Symon, K. R. and Sessler, A. M. Methods of radio frequency acceleration in fixed field accelerators with applications to high current and intersecting beam accelerators. CERN Symp. 1956. *1*, p. 44-58.
5. O'Neill, G. K. The storage-ring synchrotron. CERN Symp. 1956. *1*, p. 64-5.

6a. Nielsen, C. E. and Sessler, A. M. Longitudinal space charge effects in particle accelerators. Rev. sci. Instrum., *30*, p. 80-9, 1959.

b. Nielsen, C. E. and Sessler, A. M. Longitudinal space charge effects—phase boundary equations and potential kernels. MURA (*) 480. June 26, 1959.

7a. Vogt-Nilsen, N. Report in preparation. (CERN).

b. Reilly, D. Computer studies of beam stacking effects. MURA (*) 477. June 30, 1959.

(*) See note on reports, p. 696

8a. Robinson, K. and Ritson, D. M. Radiation coupling with betatron oscillations in circular accelerators. CAP (*)-14. November 30, 1955.

b. Robinson, K. W. Control of oscillation amplitudes. CEA (*) (USA) 4. May 15, 1956.

c. Robinson, K. W. Radiation effects in circular electron accelerators. CEA (*) (USA) 44. January 6, 1958.

d. Kolomenskij, A. A. and Lebedev, A. N. Metody podavleniya betatronnykh kolebanij v cil'no fokusiruyushchikh elektronnykh sinkhrotronakh. (Methods of reducing betatron oscillations in strong focusing electron synchrotrons). Pribory i tekh. Eksper., 1957, No. 1, p. 22-3.

e. Kolomenskij, A. A. and Lebedev, A. N. The effect of radiation on the motion of relativistic electrons in a synchrotron. CERN Symp. 1956. *1*, p. 447-55.

9a. Budker, G. J. Relativistic stabilized electron beam. I. Physical principles and theory. CERN Symp. 1956. *1*, p. 68-75.

b. Budker, G. J. and Naumov, A. A. Relativistic stabilized electron beam. II. Brief review of experimental work. CERN Symp. 1956. *1*, p. 76-9.

10. Barber, W. C., Richter, B., Panofsky, W. K. H., O'Neill, G. K. and Gittelman, B. An experiment on the limits of quantum electrodynamics. HEPL (*) 170. June 1959.

11a. Terwilliger, K. M. A radio frequency system for experiments with the FFAG electron model. MURA (*) 254. April, 1957.

b. Terwilliger, K. M., Jones, L. W. and Pruett, C. H. Radio frequency experiments with an FFAG electron model accelerator. MURA (*) 255. April 1957.

c. Terwilliger, K. M., Jones, L. W. and Pruett, C. H. Beam stacking experiments in an electron model FFAG accelerator. MURA (*) 330. 1957. *Also in:* Rev. sci. Instrum., *28*, p. 987-97, 1957.

d. Jones, L. W., Pruett, C. H., Symon, K. R. and Terwilliger, K. M. Comparison of experimental results with the theory of radio-frequency acceleration processes in FFAG accelerators. See p. 58.

12a. Cole, F. T. and Sessler, A. M. Design of a 50 MeV electron radial sector FFAG accelerator. MURA (*) 373. November 4, 1957.

b. Cole, F. T., Day, E. A., Haxby, R. O. and Sessler, A. M. Parameters and dimensions of the 50 MeV electron FFAG accelerator. MURA (*) 375. November 8, 1957.

c. Jones, L. W. Some characteristics of the 40 MeV two-way electron model. MURA (*) 396. April 10, 1958.

13. Johnston, L. H., Swenson, D. A. and Rowe, E. M. RF program for the 40 MeV two-way electron model. MURA (*) 426. August 22, 1958.

14. Parzen, G. The radiation energy loss in a fixed field accelerator. MURA (*) 376. November 14, 1957.

15. Schoch, A. Report in preparation (CERN).

16. Linhart, J. G. Accelerated self-constricted electron streams in plasma. Proc. roy. Soc. A.*249*, p. 318-34, 1959.

17a. Enoch, J. Properties of neutralized relativistic electron beams. MURA (*) 311. June, 1957.

b. Lawson, J. D. On the adiabatic self-constriction of an accelerated electron beam neutralised by positive ions. J. Electronics and Control, *3*, p. 587-94, 1957.

18. Finkelstein, D. and Sturrock, P. A. Stability of relativistic self-focusing streams. CERN PS (**) Internal Report AR 59-2. February, 1959. (Probably to appear in Drummond, J. E., Plasma physics. New York, McGraw Hill.)

19. See for instance: Paul, W. Streuung und Bremsung energiereicher Elektronen. *In:* Heisenberg, W. Kosmische Strahlung. 2. Aufl. Berlin, Springer, 1953. p. 482-94.

20. Fermi, E. Nuclear Physics. Chicago, University of Chicago Press, 1950. p. 31-4.

21. Private communication from DESY (Deutsches Elektronen-Synchrotron) Group. Hamburg.

22. Vogt-Nilsen, N. Theory of RF acceleration in fixed field circular accelerators. The concept of buckets. Moving buckets far from transition energy. CERN Internal Report PS (**)/NVN 1. February, 1958.

23. The design of quadrupole lenses for the proton synchrotron. CERN-PS (**)/MM31. March, 1957.

(*) See note on reports, p. 696.

(**) Internal memoranda not generally distributed but possibly available from author.